



Scenario approach for the seasonal forecast of Kharif flows from Upper Indus Basin

Muhammad Fraz Ismail and Wolfgang Bogacki

Department of Architectural and Civil Engineering, Koblenz University of Applied Sciences, Germany.

5

Correspondence to: W. Bogacki (bogacki@hs-koblenz.de)

Abstract. Snow and glacial melt runoff are the major sources of water contribution from the high mountainous terrain of Indus river upstream of the Tarbela reservoir. A reliable forecast of seasonal water availability for the Kharif cropping season (April – September) can pave the way towards the better water management and subsequently boost the agro-economy of Pakistan. The use of degree-day models in conjunction with the satellite based remote sensing data for the forecasting of seasonal snow and ice melt runoff has proved to be a suitable approach for the data scarce regions. In the present research, Snowmelt Runoff Model (SRM) has not only been enhanced by incorporating the “glacier (G)” component but also applied for the forecast of seasonal water availability from the Upper Indus Basin (UIB). Excel based SRM+G takes into account of separate degree-day factors for snow and ice melt processes. The UIB has been divided into Upper and Lower part because of the different climatic conditions in the Tibetan plateau. The application of seasonal scenario based approach proved to be very adequate for long term water availability forecast. The comparison between different models of operational seasonal forecasts for the UIB for the period in consideration show that SRM+G tends to slightly underestimate the flow volume on average by about 2% with an overall mean absolute error MAE of 9.6%, while the two other approaches overestimate the Kharif flow volume on average by about 6%. More important, the standard deviation of SRM+G forecast errors is 5.7% only, which is an important indicator for the forecasting skill.

10
15
20



1 Introduction

Mountains are the water towers of the world. They are the biggest resource of freshwater to half of the world's population fulfilling their needs for irrigation, industry, domestic and hydropower (Viviroli et al., 2007). The Indus River on which Pakistan's socio-economic development depends can be termed as the bread basket of Pakistan (Clarke, 2015). Due to agrarian economy, Pakistan's agriculture share in water usage is about 97%, which is well above the global average of about 70% (Akram, 2009). In Pakistan, Indus River System Authority (IRSA) decides the provincial water shares according to the Water Apportionment Accord (WAA) of 1991 and provincial irrigation departments subsequently determine the seasonal water allocation to the different canal command areas depending upon the water availability forecast carried out at the end of March for the forthcoming Kharif cropping season (April-September). A reliable seasonal forecast of the water availability from snow and glacial melt is therefore of utmost importance for the agricultural production and efficient water management.

But on the other hand snowmelt runoff modelling in mountainous regions faces the challenge of data scarcity as well as the uncertainty in parameter calibration (Pellicciotti et al., 2012). The need of the hour is to not only develop such a hydrological model which has the capability to cater both snow and glacial melt component but also a reliable forecast technique which could help the water managers and policy makers for enhancing the water resources management in future. Present paper focuses on the Upper Indus Basin (UIB) from where the major portion of water is contributed by the seasonal snow and glacial melt (Tahir et al., 2011). The ExcelSRM version (Bogacki and Hashmi, 2013) of WinSRM (Martinec et al., 2011) has been enhanced by taking into account the glacial melt component based on the methodology proposed by Schaper et al. (1999) and by introducing the possibility to split a watershed into sub-catchments which is not implemented in WinSRM. As applicable seasonal, i.e. 6 months, temperature and precipitation forecasts are not to be expected in the near future, a scenario approach that was already successfully applied in the Upper Jhelum Basin (Bogacki and Ismail, 2016) is used to predict the inflow to Tarbela reservoir for the forthcoming Kharif season.

2 Materials and Methods

2.1 Study area

The upper catchments of the Indus river basin (Figure 1) primarily feed Tarbela reservoir of Pakistan. The Upper Indus Basin has an area of 173,345 km² of which approx. 11.5% is covered by perennial glacial ice (Tahir et al., 2011). At the end of most winters nearly the entire UIB above 2,200 meters asl is covered with snow, resulting in that more than 60% of annual flow in the Upper Indus River is contributed by the snowmelt (Bookhagen and Burbank, 2010). From May to July melting of seasonal snow cover contributes to the bulk of the flow of the Upper Indus streams. The distribution of monthly inflows to the Tarbela reservoir (see Figure 2) shows that these flows tend to rise progressively as melting temperatures advance into areas of higher snowpack at higher elevations. Indus River starts rising gradually in March reaching its maximum in July, while peak flood events usually occur during monsoon season in July – September. When by the end of July the flows reduce due to diminished snow cover in the lower catchment, the high altitude glacierised basins become important contributors to the flows due to first melting of their seasonal snow cover and when the snow has vanished melting of the glacier ice. According to Tahir



et al. (2011) glacial melt dominates the flows of the largest tributaries of Indus river, i.e. Chitral, Gilgit, Hunza, Braldu and Shyok rivers.

2.2 Splitting the UIB into two sub-catchments

In the Karakorum – Western Himalayas region snow usually accumulates during winter and reaches its maximum extension during February/March. Higher altitudes typically have a 90% – 100% snow cover that stays more or less constant until temperature rises above 0°C at that elevation zone and melting starts. However, as it can be observed from the analysis of MODIS snow cover data e.g. for March and April of 2003 (Table 1), in the south-eastern part of the UIB namely the Tibetan plateau the snow cover is fading away very soon while on the other hand, in the north-western part of the catchment at the same elevation zone there remains a significant higher snow cover area.

As in SRM the estimation of the snow-water equivalent strongly depends on a correct representation of the zonal snow cover and its depletion curve, the different behaviour in the north-western and south-eastern part was accounted for by splitting the UIB into two sub-catchments at Kharhong gauging station, namely Lower and Upper UIB (see Figure 3). For each simulation, first the Upper UIB model is run in order to calculate flows at Kharhong. These flows are then superimposed to the flows calculated by the Lower UIB model using a time-lag between Kharhong and Tarbela of 3 days that was determined by the Kirpich travel-time equation.

2.3 Model Structure

In the Himalayas and its surroundings, Immerzeel et al. (2009, 2010) investigated the effects of snow cover dynamics on the discharge of the Upper Indus River and concluded that stream flows can be predicted with a high degree of accuracy using MODIS snow cover data in the snowmelt runoff model (SRM). The snowmelt runoff model (Martinec, 1975) is a semi-distributed, lumped temperature index model which is specifically designed to simulate the runoff in snow-dominated catchments that has been successfully applied in more than hundred snow-driven basins (Martinec et al., 2011). Input variables of SRM are daily values of air temperature, precipitation, and snow-covered area. If the elevation range of the catchment exceeds 500 m the catchment is subdivided into elevation zones of about 500 m each (Martinec et al., 2011). The total daily amount of water produced from snowmelt and rainfall in the catchment is superimposed on the calculated recession flow according to Equation (1):

$$Q_{n+1} = \sum_{i=1}^m \left\{ [M_{n,i} + R_{n,i}] \cdot \frac{10000}{86400} A_i \right\} \cdot (1 - k_{n+1}) + Q_n k_{n+1} \quad (1)$$

Q is average daily discharge [m^3s^{-1}], M and R the daily snowmelt and rainfall depth [cm d^{-1}], A the total area of the elevation zone [km^2], k the recession coefficient [-], n the index of the simulation day, and i and m the indices and total number of elevation zones respectively.

Daily runoff from snowmelt and rainfall is calculated by equations (2) and (3):

$$M_{n,i} = c_{Sn,i} \cdot a_{Sn,i} \cdot T_{n,i} \cdot S_{n,i} \quad (2)$$



$$R_{n,i} = c_{Rn,i} \cdot P_{n,i} \quad (3)$$

where c_S and c_R are the runoff coefficients [-] for snowmelt and rain, a_S is the degree-day factor for snow [$\text{cm } ^\circ\text{C}^{-1} \text{ d}^{-1}$], T the number of degree-days [$^\circ\text{C d}$] for each elevation zone, S the ratio of the snow covered area to the total area [-] and P the daily precipitation [cm].

Schaper et al. (1999) introduced an enhancement in the original SRM approach by incorporating the separate glacial melt component in the model. In addition to the variables used by SRM it also considers the area covered by exposed, i.e. not snow covered, glaciers. An additional melt component is added to equation (1) that takes into account the specific degree-day factors for glaciers according to equation (4):

10

$$G_{n,i} = c_{Gn,i} \cdot a_{Gn,i} \cdot T_{n,i} \cdot S_{Gn,i} \quad (4)$$

G is the daily melt [cm d^{-1}] from exposed glaciers in each elevation zone, c_G are the runoff coefficient [-] and a_G is the degree-day factor [$\text{cm } ^\circ\text{C}^{-1} \text{ d}^{-1}$] for glaciers, and S_G is the ratio of the exposed glacier area to the total area [-].

15 This model was tested in several basins and found high accuracy even in basins with 67% glacier areas on three alpine basins Rhine-Felsberg, Rhône-Sion and Ticino-Bellinzona in Switzerland (Schaper and Seidel, 2000). Apart from the improvement of the runoff modelling, the independent computation of glacier melt is an important step towards evaluations of glacier behaviour with regard to climate change.

The glacier melt component according to equation (4) was incorporated into the existing ExcelSRM resulting in 20 the new version named SRM+G. This extension requires the glacier exposed area as an additional daily input variable and respective model parameters as given in equation (4).

An additional enhancement is the possibility to split the watershed into different sub-catchments. This feature is realised by adding the pre-calculated outflow of a sub-catchment obtained by a separate simulation to the discharge of the downstream sub-catchment. The travel time can be considered by applying a time-lag to the daily discharge 25 time-series.

According to the elevation band approach of SRM, the lower and upper sub-catchments of UIB were subdivided into elevations zones of 500 m height. The hypsometric information including the number of elevation zones and their corresponding areas of both the sub-catchments are shown in Figure (4).

2.4 Model parameters

30 The most important parameter of a temperature-index model which is controlling daily snow and glacial melt is the degree-day factor [$\text{cm } ^\circ\text{C}^{-1} \text{ d}^{-1}$], which transforms the index variable degree-day [$^\circ\text{C d}$] into actual melt [cm d^{-1}]. In the first step, for the snowmelt component, best-fitting degree-day factors were obtained for each elevation zone by diagnostic calibration while the daily glacial melt depth was computed by using a constant value of 0.70 [$\text{cm } ^\circ\text{C}^{-1} \text{ d}^{-1}$] as proposed by (Schaper et al., 2000) that corresponds to degree-day factors reported from glacier in the 35 Himalayas at a comparable latitude (Hock, 2003).

As, a generalised rule is needed in the forecasting procedure, zone-wise degree-day factor functions (Ismail et al., 2015) were developed. The increase of degree-day factors versus time after the snow melting starts was plotted for each elevation zone for all calibrated years for both the catchments (Figure 5 & 6). The start of snowmelt and



correspondingly application of the developed degree-day factors generalised rule, is correlated with a certain threshold temperature for each elevation zone (Table 2 & 3). The other model parameters required by SRM like temperature lapse-rate, recession coefficient, runoff coefficient for snow, lag-time, etc., were applied basin-wide and kept constant for all years. The values of these parameters were determined according to the methods described by Martinec et al., (2011) and slightly adjusted to achieve a good fit over the whole calibration period.

2.5 Data sources

There are a number of high elevation climate stations in the Pakistani part of the Upper Indus Basin operated by WAPDA's¹ Glacier Monitoring and Research Centre (GMRC) and Pakistan Meteorological Department (PMD). However, they are concentrated on the western part of the UIB and data is not available online. In order to have most recent data for operational flow forecasting, the World Meteorological Organization (WMO) climate station at Srinagar airport located at an altitude of 1,587 m asl was chosen as temperature base station, which already had proven to give representative temperatures for that region in the SRM model of the Upper Jhelum catchment (Bogacki and Ismail, 2016) and a full set of climatic data can be obtained online from the GSOD² data-base with a time-lag of about 2 days only. Based on the daily air temperature data, degree-days in each elevation zone were calculated using a constant temperature lapse-rate of $-6^{\circ}\text{C km}^{-1}$.

The MODIS/Terra Snow Cover Daily L3 Global 500 m Grid (MOD10A1) product³ has been used to determine the daily snow covered area in the elevation zones. As the sensor cannot detect snow below clouds, a cloud elimination algorithm is applied using temporal interpolation between two cloud-free days for each pixel. Afterwards the daily percentage of snow cover area in each elevation zone is calculated and smoothed by moving average. At the beginning of the melting season, glaciers are usually completely covered by fresh snow. As the melting season progresses the snow cover will fade away and glacier exposed area will increase. The actual glacier extent was derived from two data sources. As a major source on global glacier distribution the Global Land Ice Measurements from Space (GLIMS) data archive was used (Raup et al., 2007). This data was complemented by interpretation of Landsat 8 scenes (30 m spatial resolution) from late summer to early fall 2013, in order to identify the maximum of the glacier exposed area. The merged data was mapped on the 500 m MODIS grid. On a daily basis, the glacier exposed area is determined by all pixels that are classified as glacier but not identified as snow by the MODIS sensor.

A spatial interpolation of in-situ (station) precipitation data in mountainous regions is particularly difficult and often biased towards lower values (Archer and Fowler, 2004) as the rain gauge network is usually sparse and mainly located at the valley floors while maximum precipitation occurs on mountains slopes and increases with altitude in general. A promising alternative to station data are gridded, remote sensing based precipitation products. However regional and temporal pattern as well as multiannual means of these products differ significantly in the Himalayas (Palazzi et al., 2013). In particular, the widely used TRMM 3B34 product is known to underestimate the precipitation in high altitudes as found in the UIB (Forsythe et al., 2011) or the Andes (Ward et al., 2011).

¹ Pakistan Water and Power Development Authority

² Global Summary Of the Day. Download at: <ftp://ftp.ncdc.noaa.gov/pub/data/g sod/>

³ Hall et al. (2006), updated daily. MODIS/Terra Snow Cover Daily L3 Global 500m Grid V005, [Feb. 2000 – Sep. 2016, tiles h23v05 & h24v05]. NSIDC Boulder, Colorado USA. Download at: <ftp://n5eil01u.ecs.nsidc.org/SAN/MOST/MOD10A1.005>



Based on own precipitation product comparisons for the Upper Chenab catchment, the gridded RFE 2.0 Central Asia⁴ daily rainfall product (Xie et al., 2002) is used in the present model. According to SRM's elevation band approach, the gridded data, having a spatial resolution of 0.1° latitude/longitude, is mapped to the respective elevation zones. For the period 2003 – 2015 the product yields a mean annual precipitation of 854 and 482 mm/a for the Lower and the Upper UIB respectively, that reflects the significantly lower annual precipitation on the Tibetan plateau compared to the western Himalayas (e.g. Bookhagen and Burbank, 2010; Ménégoz et al., 2013). The RFE basin-wide annual mean of 701 mm/a lies well in the range of 675 ±100 mm/a derived for the whole UIB by Reggiani and Rientjes (2014).

2.6 Scenario approach for forecasting

- 10 In the forecasting phase which starts from the 1st of April, the four model variables temperature, precipitation, snow covered area and glacier exposed area have to be predicted for the forthcoming 6 months of the Kharif cropping season (April – September). As the level of skill of seasonal climate forecasts for the Hindukush – Karakoram – Western Himalaya region for such a lead time is still not sufficient, a scenario approach already successfully applied in the Upper Jhelum catchment (Bogacki and Ismail, 2016) is used.
- 15 In order to estimate the future depletion of the snow-covered area, SRM uses so-called “modified depletion curves” which are derived from the conventional depletion curves of each elevation zone by replacing the time scale with the cumulative daily snow-melt depth (Martinec et al., 2011). The decline of the modified depletion curves depends on the initial accumulation of snow and represents the actual snow-water equivalent. When initial snow depth is low the modified depletion curve declines faster than in years when a lot of snow has accumulated. In the end of
- 20 March, when the seasonal forecast is carried out, an elevation zone showing already some decline in snow covered area, and hence having also some cumulated degree-days, is chosen as “key zone”. Comparing the relation of decline in snow covered area versus cumulated degree-days with a statistical analysis of the modified depletion curves of previous years, the actual amount of snow is estimated and the future depletion anticipated accordingly, while assuming similar snow conditions for all elevation zones.
- 25 While the snow-covered area and its depletion is calculated on basis of the actual snow conditions, scenario runs are carried out with observed temperature, precipitation, and glacier exposed area data-sets of historic years. In this scenario approach, the respective data of each historic year is considered as one scenario. Simulation runs for all years result in an ensemble of predicted seasonal flows representing historic weather conditions from which by statistical analysis a forecast of “most likely” (median) as well as expected flows under “dry” (20%) and “wet”
- 30 (80%) probability of occurrence are derived.

3 Results and discussion

The final flow forecast models, i.e. using fixed model parameters as well as the developed degree-day factor functions and the start rule as shown in Table 2 & 3, was validated for the series of years 2003 – 2012. The relative

⁴ RainFall Estimates version 2.0 created by the NOAA Climate Prediction Center's FEWS-NET group sponsored by USAID. Download at: <ftp://ftp.cpc.ncep.noaa.gov/fews/afghan>



volume difference D_v and the Nash- Sutcliffe coefficient of determination R^2 were calculated according to the Eq. (5) and Eq. (6):

$$D_v = \frac{V - V^*}{V} \times 100 [\%] \quad (5)$$

$$R^2 = 1 - \frac{\sum_{i=1}^n (Q_i - Q_i^*)^2}{\sum_{i=1}^n (Q_i - \bar{Q})^2} \quad (6)$$

5 These equations are used as model accuracy criteria, where V and V^* are the observed and the simulated annual flow volumes, Q_i and Q_i^* are the observed and the simulated daily discharge values, and \bar{Q} is the average observed daily discharge.

The total series of years has an average R^2 of 0.93 and 0.87 as well as average absolute volume error of -3.7% and -1.0% for both Upper and Lower UIB model respectively. Examples of simulated versus observed inflow
10 hydrograph are given in Figure 7 & 8.

The forecast skill of the developed model was evaluated by hind-casts for the years 2003 – 2014 using the same procedures as developed for the operational seasonal forecasts with an overall mean absolute error MAE of 9.6%. Meanwhile, real forecasts for the Kharif seasons of the years 2015 and 2016 are available with an absolute error of 12.3% and 5.0% respectively. Results are also compared with IRSA's statistical forecasts and with forecasts from
15 the UBC⁵ watershed model (Quick and Pipes, 1977) that is used by WAPDA's Glacier Monitoring Research Centre. The comparison of the relative error of the forecasted Kharif flow volumes by the different approaches in Table 4 shows that SRM+G tends to slightly underestimate the flow volume on average by about 2% while the two other approaches overestimate the Kharif flow volume on average by about 6%. Although there is not much room for improvement taking the excellent mean absolute error of IRSA's statistical approach, this value could be
20 reduced by SRM+G to less than 10% for the period in consideration. More important, the standard deviation of SRM+G forecast errors is 5.7% only, which is an important indicator for the forecasting skill.

The splitting of UIB into upper and lower part proved to be a necessary approach in terms of improving the flow forecasting. The snowpack melting behaviour as well as precipitation pattern on the Tibetan plateau is substantially different from the north-western part and it should be handled separately.

25 The use of a gridded precipitation product that adequately reflects the mean annual precipitation depth was well as its regional variations, although it sometimes over- or underestimates a single rainfall event considerably, might also be favourable in that context as the spatial distribution seems to be more fitting as any interpolation of station data in such mountainous regions.

In order to further improve the seasonal forecast skill of the scenario approach, research is under way on the early
30 identification of cold/warm respectively dry/wet years e.g. correlated to the ENSO⁶ status or other potential teleconnections, which might allow for a more specific selection of a subset of corresponding historic years.

⁵ University of British Columbia Watershed Model

⁶ El Niño Southern Oscillation



Acknowledgements

The authors thank National Engineering Services Pakistan (Pvt.) Ltd. (NESPAK), Lahore and AHT Group AG, Essen, Germany that they could be part of the project team. They are highly grateful to Indus River System Authority (IRSA) and WAPDA's Glacier Monitoring Research Centre (GMRC) and Surface Water Hydrology 5 Project (SWHP) of for sharing their forecast results as well as the daily discharge data.

References

- Akram, A. A.: Indus Basin water resources, *Tiempo*, Issue 70., <http://www.environmentportal.in/files/Indus%20Basin.pdf>, 2009.
- 10 Archer, D. R. and Fowler, H. J.: Spatial and temporal variations in precipitation in the Upper Indus Basin, global teleconnections and hydrological implications, *Hydrol. Earth Syst. Sci.*, 8, 47–61, doi:10.5194/hess-8-47-2004, 2004.
- Bogacki, W. and Hashmi, D.: Impact of Climate Change on the Flow Regime of the Mangla Basin. GWSP Conference 'Water in the Anthropocene: Challenges for Science and Governance. Indicators, Thresholds and 15 Uncertainties of the Global Water System, Bonn, http://conference2013.gwsp.org/uploads/media/Bogacki_Impact_of_Climate_Change_on_the_Flow_Regime_of_the_Mangla_Basin.pdf, 2013.
- Bogacki, W. and Ismail, M. F.: Seasonal forecast of Kharif flows from Upper Jhelum catchment. In Proc. IAHS 374, pp. 137–142. DOI: 10.5194/piahs-374-137-2016.
- 20 Bookhagen, B. and Burbank, D.W.: Toward a complete Himalayan hydrological budget: Spatiotemporal distribution of snowmelt and rainfall and their impact on river discharge, *J. Geophys. Res.*, 115, F03019, doi:10.1029/2009JF001426, 2010.
- Clarke, M.: Climate Change Considerations for Hydropower Projects in the Indus River Basin, Pakistan. Impact Assessment in the Digital Era, 35th Annual Conference of the International Association for Impact Assessment, 25 Italy, 2015.
- Forsythe, N., Fowler, H. J., Kilsby, C. G. and Archer, D. R.: Opportunities from remote sensing for supporting water resources management in village/valley scale catchments in the Upper Indus Basin. *Water Resour. Manage.* 26 (4), 845–871, 2011.
- Hock, R.: Temperature index melt modelling in mountain areas. *Journal of Hydrology* 282, 104–115, 2003.
- 30 Immerzeel, W.W., van Beek, L.P.H. and Bierkens, M.F.P.: Climate change will affect the Asian water towers. *Science*, 328(5984): 1382–1385, 2010.
- Immerzeel, W.W., Droogers, P., de Jong, S. M., and Bierkens, M. F. P.: Large-scale monitoring of snow cover and runoff simulation in Himalayan river basins using remote sensing, *Remote Sensing of Environment*, 113, 40–49, doi:10.1016/j.rse.2008.08.010, 2009.
- 35 Ismail, M. F., Rehman, H., Bogacki, W., and Noor, M.: Degree Day Factor Models for Forecasting the Snowmelt Runoff for Naran Watershed, *Sci. Int. Lahore*, 27(3), 1961–1969, 2015.
- Martinec, J., Rango, A., and Roberts, R.: Snowmelt Runoff Model User's Manual, WinSRM Version 1.14. Agricultural Experiment Station Special Report 100, New Mexico State University, Las Cruces, NM 88003, USA, 2011.
- 40 Martinec, J.: Snowmelt-Runoff Model for Stream Flow Forecasts, *Nord. Hydrol.*, 6, 145–154, 1975.
- Ménégoz, M., Gallée, H. and Jacobi, H. W.: Precipitation and snow cover in the Himalaya: from reanalysis to regional climate simulations. *Hydrol. Earth Syst. Sci.* 17, 3921–3936, 2013.
- Palazzi, E., Hardenberg, J. and Provenzale, A.: Precipitation in the Hindu-Kush Karakoram Himalaya: Observations and future scenarios, *J. Geophys. Res. Atmos.*, 118, 85–100, doi: 10.1029/2012JD018697, 2013.
- 45 Pellicciotti, F., Buergi, C., Immerzeel, W. W., Konz, M., and Shrestha, A. B.: Challenges and Uncertainties in Hydrological Modeling of Remote Hindu Kush–Karakoram–Himalayan (HKH) Basins. Suggestions for



- Calibration Strategies. In Mountain Research and Development 32 (1), pp. 39–50. DOI: 10.1659/MRD-JOURNAL-D-11-00092.1, 2012.
- Quick, M. C. and Pipes, A.: UBC watershed model, *Hydrol. Sci. Bull.*, 221, 153–161, 1977.
- Raup, B.H., Racoviteanu, A. Khalsa, S.J.S. Helm, C. Armstrong, R. and Arnaud Y.: "The GLIMS Geospatial
5 Glacier Database: a New Tool for Studying Glacier Change". *Global and Planetary Change* 56:101–110, 2007.
- Reggiani, P. and Rientjes, T. H. M.: A reflection on the long-term water balance of the Upper Indus Basin. *Hydrol. Res.*, 46(3), 446-462, DOI:10.2166/nh.2014.060, 2015.
- Schaper J, Seidel K.: Modelling daily runoff from snow and glacier melt using remote sensing data. In Proceedings of the 2nd EARSel Workshop—Special Interest Group Land Ice and Snow (pp. 308-316), 2000.
- 10 Schaper, J., Martinec, J., And Seidel, K.: Distributed Mapping of Snow and Glaciers for Improved Runoff Modelling. *Hydrological Processes*, 13(12-13): 2023–2031, 1999.
- Schaper, J. Seidel, K., and Martinec, J.: Precision snow cover and glacier mapping for runoff modelling in a high alpine basin. *IAHS Publ. no. 267*, 2001, 105–111, 2000.
- Tahir, A. A.; Chevallier, P.; Arnaud, Y.; Ahmad, B.: Snow cover dynamics and hydrological regime of the Hunza
15 River basin, Karakoram Range, Northern Pakistan. *Hydrol. Earth Syst. Sci.* 15 (7), pp. 2275–2290. DOI: 10.5194/hess-15-2275-2011.
- Viviroli, D. Dürr, H. H. Messerli, B. Meybeck, M., and Weingartner, R.: Mountains of the world, water towers for humanity. Typology, mapping, and global significance. *Water Resour. Res.* 43 (7). DOI: 10.1029/2006WR005653, 2007.
- 20 Ward, E., Buytaert, W., Peaver, H., and Wheat, L.: Evaluation of precipitation products over complex mountainous terrain: A water resources perspective. *Adv. Water Resour.* 34 (10), 1222–1231, 2011.
- Xie, P. Yarosh, Y. Love, T. Jonowiak, J.E., and Arkin, P.A.: A real-time daily precipitation analysis over south asia. Preprint of the 16th Conference on Hydrology, Orlando, Florida. American Meteorological Society, Washington DC, USA. http://www.cpc.ncep.noaa.gov/products/fews/sasia_rfe.pdf, 2002.
- 25

Reggiani, P. and T.H.M. Rientjes (2015). A reflection on the long-term water balance of the Upper Indus Basin, *Hydrology Research*, 46(3), 446-462, DOI:10.2166/nh.2014.060



Table 1: Comparison of snow cover area at the same elevation for Upper and Lower part of UIB

| March – 2003 | | | | | | |
|--------------|------|------|------|------|------|-------|
| Elevation | 3500 | 4000 | 4500 | 5000 | 5500 | >5500 |
| Lower UIB | 66% | 82% | 88% | 87% | 83% | 94% |
| Upper UIB | 58% | 79% | 58% | 51% | 58% | 71% |
| April – 2003 | | | | | | |
| Lower UIB | 42% | 71% | 84% | 84% | 78% | 92% |
| Upper UIB | 24% | 50% | 48% | 43% | 51% | 73% |

Table 2: Zone-wise degree-day factors and 10-daily temperature threshold depending on 10-days periods after melting start for Lower UIB

| 10-daily Period | Elevation Zone | | | | | | | |
|--------------------|----------------|------|------|------|------|------|------|-------|
| | 0-2500 | 3000 | 3500 | 4000 | 4500 | 5000 | 5500 | >5500 |
| T_{10d}^7 | 9.0 | 7.0 | 5.0 | 4.0 | 2.0 | 1.0 | 1.0 | 1.0 |
| 1 | 0.20 | 0.21 | 0.22 | 0.22 | 0.19 | 0.18 | 0.18 | 0.20 |
| 2 | 0.30 | 0.32 | 0.32 | 0.32 | 0.30 | 0.31 | 0.31 | 0.33 |
| 3 | 0.39 | 0.43 | 0.41 | 0.43 | 0.41 | 0.43 | 0.44 | 0.46 |
| 4 | 0.48 | 0.53 | 0.51 | 0.54 | 0.52 | 0.56 | 0.57 | 0.59 |
| 5 | 0.57 | 0.64 | 0.61 | 0.65 | 0.63 | 0.68 | 0.70 | 0.72 |
| 6 | 0.67 | 0.75 | 0.70 | 0.80 | 0.74 | 0.80 | 0.80 | 0.80 |
| 7 | 0.80 | 0.80 | 0.80 | 0.80 | 0.80 | | | |

5

Table 3: Zone-wise degree-day factors and 10-daily temperature threshold depending on 10-days periods after melting start for Upper UIB

| 10-daily Period | Elevation Zone | | | | | | |
|--------------------|----------------|------|------|------|------|------|-------|
| | 3000 | 3500 | 4000 | 4500 | 5000 | 5500 | >5500 |
| T_{10d} | 2.0 | 2.0 | 2.0 | 2.0 | 0.5 | 0.5 | 0.5 |
| 1 | 0.37 | 0.35 | 0.35 | 0.52 | 0.56 | 0.48 | 0.60 |
| 2 | 0.43 | 0.40 | 0.40 | 0.59 | 0.64 | 0.54 | 0.70 |
| 3 | 0.49 | 0.45 | 0.46 | 0.66 | 0.73 | 0.80 | 0.80 |
| 4 | 0.54 | 0.51 | 0.51 | 0.73 | 0.80 | | |
| 5 | 0.60 | 0.56 | 0.56 | 0.80 | | | |
| 6 | 0.66 | 0.61 | 0.62 | | | | |
| 7 | 0.71 | 0.66 | 0.67 | | | | |

⁷ 10-Daily average temperature in °C in each elevation zone.



Table 4: Statistics of relative error [%] of Kharif flow volume forecasts for the period 2003 – 2016 by IRSA’s statistical approach, UBC watershed model, and SRM+G. SRM+G 2003 – 2014 results are hind-casts, all other forecasts.

| | IRSA | UCB WM | SRM+G |
|---------------------|------|--------|-------|
| Bias | 5.8 | 6.3 | -2.1 |
| Mean absolute error | 10.9 | 11.4 | 9.4 |
| Standard deviation | 8.0 | 6.8 | 5.7 |

5

10

15

20

25

30

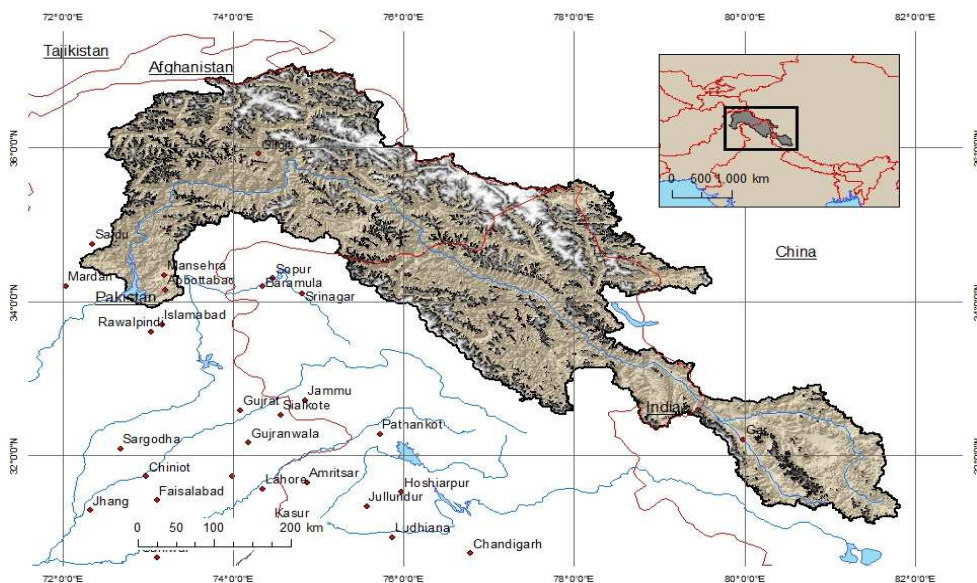
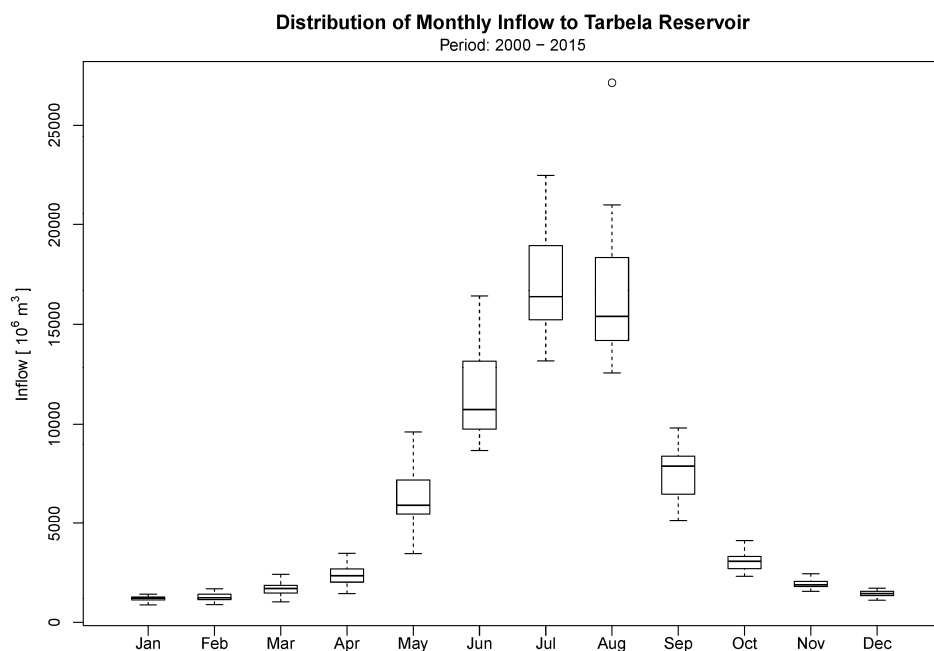


Figure 1: Map of the Upper Indus Basin showing its extent across Pakistan, India and China



5 Figure 2: Monthly distribution of inflows to the Tarbela Reservoir from 2000 - 2015

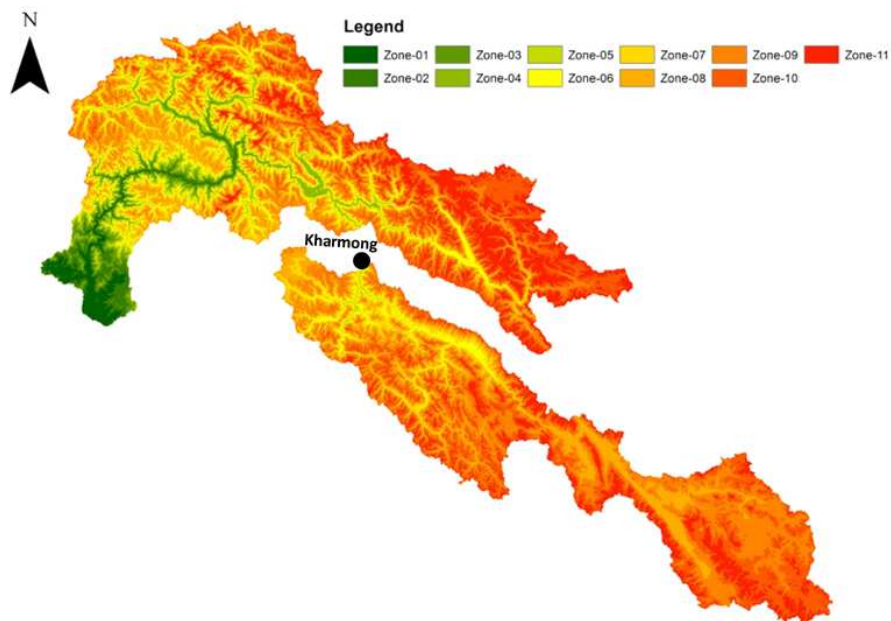


Figure 3: Splitting of Upper Indus Basin at the Kharmonig gauging station into Upper and Lower UIB

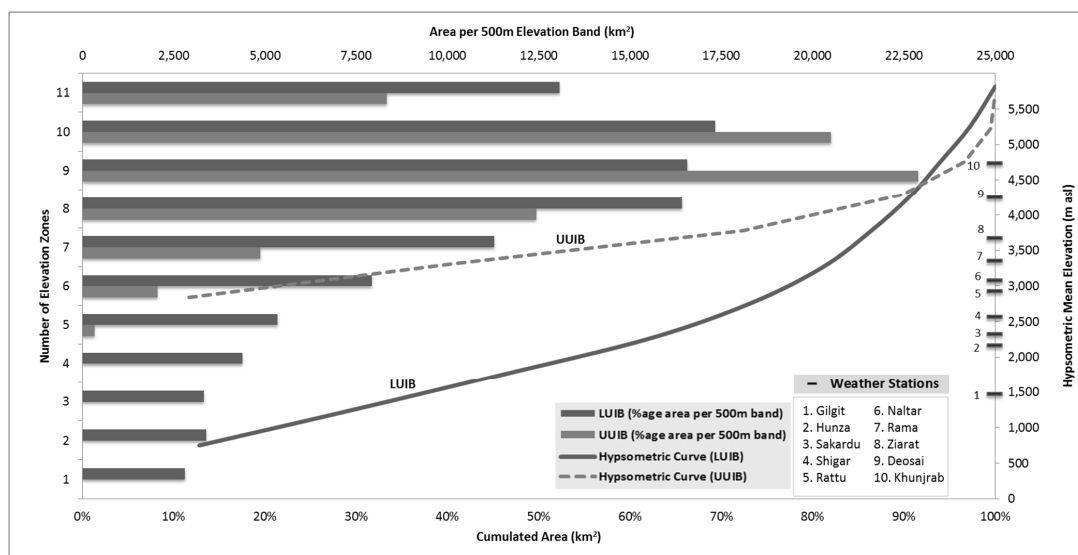


Figure 4: Hypsometric curves and the distribution of area under 500-m elevation bands for the Upper and Lower UIB. Eleven as well as seven elevation zones were made for Upper and Lower UIB and the elevation of the weather stations in western portion of the UIB are presented on the right hand side y-axis.

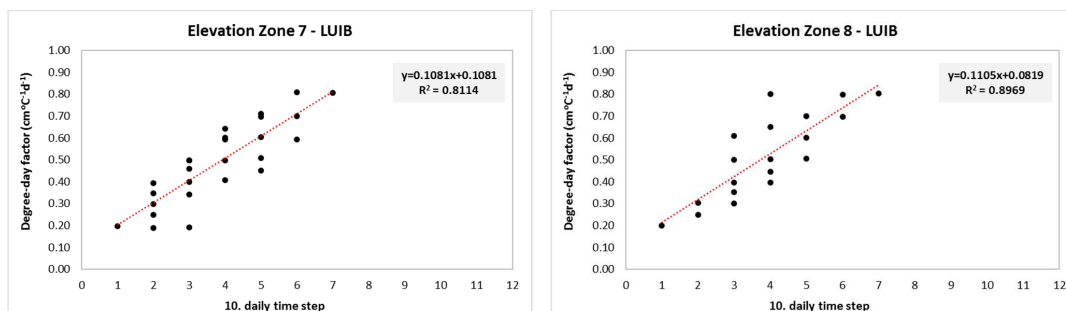
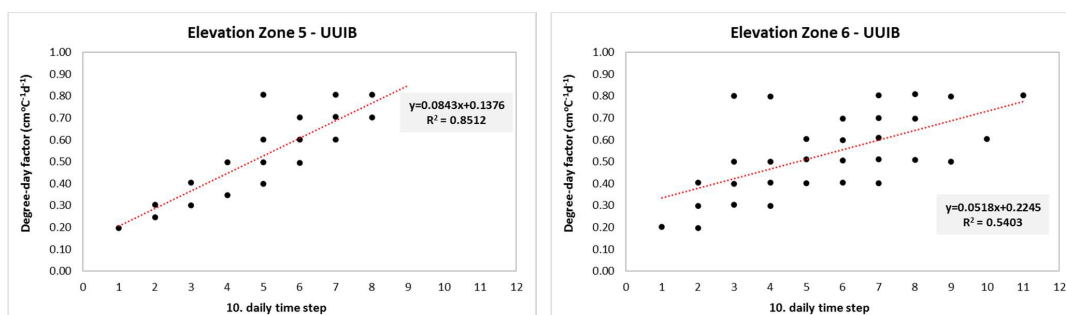


Figure 5: Increase of degree-day factors with time (10-days periods) after melting start for elevation zones 7 and 8 for Lower UIB. Degree-day factors are obtained by diagnostic calibration.



5 Figure 6: Increase of degree-day factors with time (10-days periods) after melting start for elevation zones 5 and 6 for Upper UIB. Degree-day factors are obtained by diagnostic calibration.

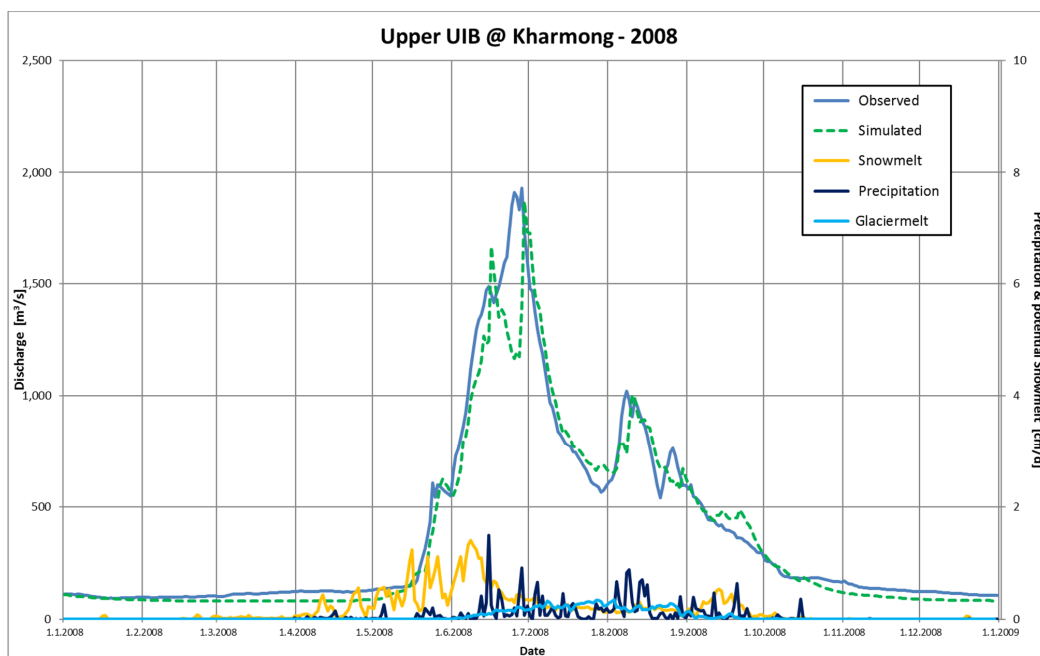


Figure 7: Results of validation of final Upper UIB flow forecast model (dashed line) compared to observed flows at Kharmong (solid line) for the year 2008. The graph also shows at the bottom rainfall, snowmelt, and glaciermelt depth [cm d⁻¹].

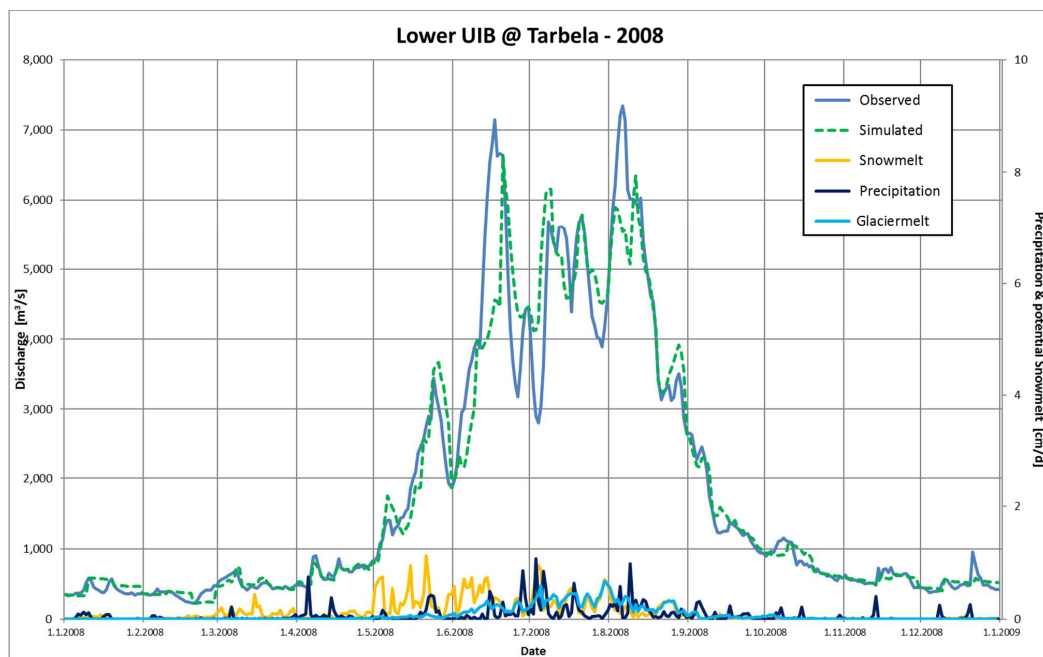


Figure 8: Results of validation of final Lower UIB flow forecast model (dashed line) compared to observed inflows at Tarbela (solid line) for the year 2008. Note that observed Tabela inflows are reduced by Kharmong flows with a lag-time of 3 days. The graph also shows at the bottom rainfall, snowmelt, and glaciermelt depth [cm d⁻¹].